Coupling lead isotope ratios and multi-element analysis from particulate matter and lichens from the Athabasca Oil Sands Region to identify local, regional, and global source contributions

Joseph R. Graney[1*], Matthew S. Landis[2], Eric S. Edgerton[3]

[1]Geological Sciences and Environmental Studies, Binghamton University, Binghamton, NY, USA
[2]Integrated Atmospheric Solutions, LLC., Cary, NC, USA
[3]Atmospheric Research & Analysis, Inc., Cary, North Carolina, USA

[*]Corresponding author; phone: (607) 777-6347; jgraney@binghamton.edu

Abstract

Ambient air particulate matter was collected at the Wood Buffalo Environmental Association (WBEA) AMS-1 Fort McKay monitoring station in the Athabasca Oil Sand Region (AOSR) in Alberta, Canada from February 2010 to July 2011. Daily twenty-four hour integrated fine ($PM_{2.5}$) and coarse ($PM_{10-2.5}$) particulate matter was collected using a sequential dichotomous sampler. A subset of 100 filter pairs were selected for element and Pb isotope analysis to determine short term variation in source contributions. Pb isotope results from 120 lichen samples collected in 2008 were analyzed to examine longer term source contributions. The results from measurements of $^{206}Pb/^{207}Pb$ and $^{208}Pb/^{207}Pb$ isotope ratios were used to identify local regional and global sources in the PM and lichen data sets. The key for identifying the global source was the recognition of thorogenic Pb from western Asia in three isotope $^{206}Pb/^{207}Pb$ versus $^{208}Pb/^{207}Pb$ plots. If one combines the results from the coarse and fine PM, contributions from China (34.4%) exceed those from mixed sources of fine PM from the AOSR (19.7 %), regional western Canada sources of fine PM (19.0%), coarse PM from haul and access roads (10.2%), oil sands (9.4%) and tailings sand (7.3%) sources. Regional sources contribute 51.7% of the Pb in the lichens, local sources 27.8% and global sources 20.6%. If the mixing model results from the proximal lichens (0-30 km) and distal lichens (30-160 km) are separated, local and regional sources predominate at the proximal sites, and global sources are more important at the distal sites. It is remarkable that we could identify and quantify the amount of this global transport signature in a location within the footprint of the world's largest concentration of bitumen mining and upgrading facilities.

Keywords: Pb isotopes, Particulate Matter, Fugitive Dust, Asian Sources, Global Transport

Introduction

The Athabasca Oil Sands Region (AOSR) in northern Alberta, Canada contains the world's largest concentration of bitumen production and upgrading facilities with economically recoverable petroleum reserves estimated to be approximately 170 billion barrels (Attanasi and Meyer, 2010; Alberta Energy Regulator, 2015). Quantifying ambient particulate matter (PM) concentrations and atmospheric deposition from this large scale industrial activity is essential for emission mitigation strategies in the AOSR from human and ecosystem health concerns. Landis et al. (2017) quantified the ambient $PM_{2.5}$ (fine) and $PM_{10\text{-}2.5}$ (coarse) concentrations and sources from 100 sets of PM collected in 2010 -2011 within the Fort MacKay First Nation community in the AOSR using positive matrix factorization (PMF) techniques. Fort Mackay is located centrally within the footprint of the AOSR surface mining operations (Figure 1). A $PM_{2.5}$ Pb factor was identified by PMF that had a pronounced seasonality component with enhanced contributions during the spring of 2010 and the spring of 2011. This seasonal pattern did not appear to be correlated with known emissions from local or regional sources, but is consistent with previously observed trans-Pacific transport of pollution from Asia to western North America (Yienger et al., 2000; VanCuren et al., 2002; VanCuren, 2003). Based on multi-element studies long range transport to the North Pacific region and adjacent land masses in western North America can include large contributions from western Asian sources superimposed over local sources (Uematsu et al., 1983; Jaffe et. al., 1999; Zdanowicz, 2006; Osterberg et al., 2008) with the contributions from western Asian sources enhanced in the springtime (Fischer et al., 2009).

It is known that lead can be emitted into the atmosphere by high temperature anthropogenic processes including non-ferrous metal smelting, battery recycling, coal combustion, waste incineration, and transportation fuels (U.S. EPA, 2015). Once emitted, lead may be transported on local, regional, or intercontinental scales depending on several factors, including particle size, the elevation of emission, and meteorology. We hypothesized that Pb isotope analysis could be used in consort with multi-element measurements to quantify contributions from Pb sources on local, regional, and global scales in the AOSR. Pb has four major isotopes, 204, 206, 207, and 208. ^{208}Pb is formed from the radioactive decay of ^{232}Th, ^{207}Pb from ^{235}U, and ^{206}Pb from ^{238}U. ^{204}Pb is referred to as common Pb (has no radioactive parent, and is much less abundant than the other isotopes). The uranium and thorium parents have differing decay rates resulting in predictable changes in Pb isotope ratios (Faure, 1986). The Pb isotope ratios from source materials can reflect the age at which Pb was incorporated into the parent material (e.g., ore deposit, coal, oil,) which is preserved without fractionation during the subsequent process that

67 emitted the Pb into the environment (Graney et al., 1995). Following emission from high temperature
68 processes such as smelting, coal combustion, or oil refining, Pb species typically nucleate or condense
69 onto atmospheric aerosols very quickly.

70 Recent particulate matter studies indicate that after the phasing out of the use of leaded gasoline in
71 China (Zheng et al., 2004; Chen et al., 2005; Wang et al., 2006), energy generation processes,
72 predominantly coal combustion, are the major source of Pb emissions to the atmosphere with smaller
73 contributions from metal refining (Chen et al. 2008; Kong et al., 2011; Li et al., 2012). The atmospheric
74 emissions from China are characterized by lead from thorogenic sources (Mukai et al., 1993, 1995;
75 Bellis et al., 2005, Cheng and Hu, 2010) which results in higher $^{208}Pb/^{207}Pb$ and $^{208}Pb/^{206}Pb$ than lead
76 from other sources (Bollhofer and Rossman, 2001, Tan et al., 2006). Thorogenic Pb contributions
77 identified in Pb isotope studies have been used to identify transboundary pollution contributions from
78 China to lake sediment in Japan (Hosono et al., 2016), the North Pacific (Gallon et al., 2011) and
79 aerosols in the western United States (Ewing et al., 2010) as well as ice cores in western Canada (Gross
80 et al., 2012) and Greenland (Bory et al., 2014). Pb isotopes have been used to document regional and
81 local emission, transport, and deposition processes using lichens in western Canada (Simonetti et al.,
82 2003) and the AOSR (Graney et al., 2012) but a thorogenic component representing long distance
83 transport has yet to be recognized in the AOSR.

84 Based on the results from metal accumulation in peat cores in the AOSR, Shotyk et al. (2017)
85 recommended that long range transport needed to be considered in source assessments. Lichens (as well
86 as peat cores) integrate deposition over long time scales (several years), so to better determine what
87 proportion of the lead in the PM in the AOSR is from Asian sources rather than regional or local sources
88 shorter sampling intervals may be needed. This paper follows up on the recommendation of Shotyk et
89 al. (2017) by merging multi-element PM data sets with Pb isotope measurements to help distinguish
90 between aerosol sources. We anticipated the use of Pb isotope ratios from daily PM samples coupled
91 with findings from lichens could provide both short and long term temporal resolution for quantifying
92 PM sources from local, regional, and global sources. Whether a thorogenic Asian lead source can be
93 identified in particulate matter collected from a remote area in western Canada superimposed over the
94 industrial fingerprint associated with oil sands processing was a goal of this study. We will demonstrate
95 that a coupled multi-element and Pb isotope approach can be used to quantify an Asian anthropogenic
96 Pb signal in the AOSR.
97

Methods

Sampling Site

The Wood Buffalo Environmental Association (WBEA) AMS-1 Bertha Ganter-Fort McKay ambient air monitoring station (57°11'21.70" N; -111°38'26.06" W) is located in the Fort McKay First Nation and Metis community. The AMS-1 site is located in an area that is in close proximity to ongoing oil sand production operations such as mining, separating, and upgrading of bitumen (Figure 1). Twenty-four hour ambient PM samples for mass and element determinations were collected on a daily basis from February 22, 2010 through July 27, 2011 using a ThermoScientific Model 2025D Sequential Dichotomous air sampler (a U.S. EPA designated Federal Equivalent Method for $PM_{2.5}$). The dichotomous sampler had a PM_{10} impactor inlet operating at 16.7 LPM to make the initial particle size cutoff at 10 μm mass median aerodynamic diameter (MMAD). The virtual impactor in line after the PM_{10} impactor inlet acts as a dichotomous splitter and dynamically segregates the particles into fine (≤ 2.5 μm) and coarse (10 – 2.5 μm) size fractions (Loo and Cork, 1998). The $PM_{2.5}$ and $PM_{10\text{-}2.5}$ size fractions were collected onto two separate 47 mm MTL Teflon filters (Measurement Technologies Laboratories, Minneapolis, MN) with Teflon support rings. Calibrated mass flow controllers maintained the fine particle filter flow at 15.0 LPM and the coarse particle filter flow at 1.67 LPM to ensure the correct MMAD size cut.

The use of a virtual impactor results in the collection of all coarse mode particles from the total flow and the fine mode particles in the minor flow on the coarse filter (Mc Farland et al., 1978). As a result, the fine mode and corrected coarse mode concentrations (mass and elements) are adjusted for this contribution using equation 1 and 2, respectively.

$$C_{Fine} = \left(\frac{M_{Fine}}{V_{Fine}}\right) \quad (1)$$

$$C_{Coarse} = \left[\frac{M_{Coarse} - \left(\frac{M_{Fine} * V_{Coarse}}{V_{Fine}}\right)}{V_{Total}}\right] \quad (2)$$

Where: C_{Fine} = Concentration $PM_{2.5}$ (μg m^{-3})
C_{Coarse} = Concentration PM_{Coarse} (μg m^{-3})
V_{Fine} = Volume of Air Through $PM_{2.5}$ Filter (m^{-3})
V_{Coarse} = Volume of Air Through PM_{Coarse} Filter (m^{-3})
V_{Total} = Volume of Air Through Sampler (m^{-3})
M_{Fine} = Mass on Fine Filter (μg)
M_{Coarse} = Mass on Coarse Filter (μg)

Further details of the pre and post filter weighing, sample collection and shipment protocols performed by ARA Inc. (Atmospheric Research & Analysis, Inc., Cary, North Carolina, USA) are found in Landis et al., 2017.

Filter Selection for Element and Pb Isotope Analysis

Over the course of the study 392 valid daily dichotomous $PM_{2.5}$ and $PM_{10-2.5}$ sample pairs were collected with mean concentrations of 6.8 ± 12.9 μg m^{-3} (mean ± standard deviation) and 6.9 ± 5.9 μg m^{-3}, respectively. A subset of 100 dichotomous sample pairs was selected for element and Pb isotope analysis. The selected samples included an even distribution across the seasons.

Teflon Filter Extraction and Trace Element Analysis

The dichotomous sampler filters were digested using a CEM Corporation (Matthews, NC) Mars Express microwave digestion system in a mixture of ultra-pure H_2O_2, HF and HNO_3 in a procedure similar to that developed by Jalkanen and Hasanen (1996). The digestion involved heating the samples in 5 ml of the mixed acid mixture at 180°C for 40 minutes (Edgerton et al., 2012). After the sample extracts had cooled, American Society of Testing and Materials (ASTM) Type I ultrapure (18.2 MΩ·cm) water was added to each vessel to bring the extract up to a final volume of 15 ml. A 25-30 mg aliquot of NIST SRM 1633c was also digested with each batch of 30-35 filters to determine extraction efficiency. Further details of the digestion procedure are provided in Edgerton et al., 2012.

The sample extracts were then analyzed for a suite of elements using a Perkin-Elmer (Waltham, MA) Model 9000 Elan-II dynamic reaction cell inductively coupled plasma mass spectrometry (DRC-ICPMS). The samples were introduced into the DRC-ICPMS by pneumatic nebulization. Peak characteristics for each target element were considered in the method to eliminate interferences from polyatomic ions derived from the plasma gas, reagents, or sample matrix. Instrument drift and suppression, or enhancement of instrument response caused by the sample matrix, was corrected by internal standardization (Edgerton et al., 2012). Target isotopes and study specific MDLs, and a summary of the DRC-ICPMS analytical results for the 100 $PM_{2.5}$ and $PM_{10-2.5}$ samples were published in Landis et al. 2017.

Pb Isotope Ratio Analysis

Aliquots of the filter digests that had been used for the multi-element determinations were subsequently

161 measured for stable Pb isotopes using a Thermo Scientific (Franklin, Massachusetts, USA) model
162 Element2 inductively coupled plasma high resolution magnetic sector field mass spectrometer (ICP-
163 SFMS). The method used to measure the Pb isotope ratios in has been described in detail in Graney et
164 al. (2012), and included: (i) self-aspiration of sample through a cyclonic spray chamber with an uptake
165 rate of 200 $\mu l\ min^{-1}$ to maximize signal stability; (ii) optimization of the detector dead time in the
166 scanning speed operation mode; (iii) utilization of low resolution detection mode to produce flat- topped
167 peak shapes; and (iv) use of a narrow mass width window (10% of the peak top-width) scanned at a high
168 sweep rate. A bracketing technique was used to correct for mass bias during the Pb isotope ratio
169 measurements using NIST SRM 981 (Krachler et al., 2004; Yip et al., 2008). The average of the Pb
170 isotope ratios from the NIST SRM 981 bracketing samples was then used to correct the results from the
171 replicate analyses for ICP-SFMS mass bias (Krachler et al., 2004; Graney et al., 2012).
172
173 **Results and Discussion**
174 ***Fort McKay Ambient Dichotomous Sample Element Results***
175 The subset of 100 dichotomous sample pairs selected for element and Pb isotope analysis had an average
176 $PM_{2.5}$ of 8.6 ± 21.6 $\mu g\ m^{-3}$ and $PM_{10\text{-}2.5}$ of 7.6 ± 5.8 $\mu g\ m^{-3}$ with the temporal variability presented in
177 Figure 2a. The concentration of Pb was typically greater in the fine than coarse fraction, and Pb
178 concentration in the fine PM was notably higher in April – May 2010 and January – May 2011 (Figure
179 2b). In contrast the S and Al concentrations showed more variability on a day to day basis (Figure 2cd),
180 with S concentrations much higher in the fine than coarse PM, and the Al concentrations higher in the
181 coarse than the fine PM. This suggests that the source(s) of the Pb are partially decoupled from the PM,
182 S, and Al sources.

183 PM studies indicate that the Pb concentration in aerosols collected in China can be as much as a factor
184 of 100 greater than those measured in Ft. McKay. Pb concentrations as high as several hundred $ng\ m^{-3}$
185 have recently been reported in several locations in China (Schleicher et al., 2011; Widory et al., 2010;
186 Wang et al., 2015; Zhou et al., 2016) versus the several $ng\ m^{-3}$ typical in Ft. MacKay (this study).
187 Because the Pb concentrations in aerosols at Ft. McKay from local sources are low, it may be feasible to
188 determine contributions from local, regional and global sources through coupled source apportionment
189 and Pb isotope ratio results.

190 Application of the U.S EPA positive matrix factorization (PMF) receptor model on the same 100 pairs
191 of Fort McKay PM used for the Pb isotope ratio measurements in this study resolved six $PM_{10\text{-}2.5}$

192 sources which explained 99% of the mass including fugitive dust from haul roads, oil sands, and mixed
193 sources as well as biomass combustion, and mobile sources (Landis et al., 2017). 40% of the $PM_{10-2.5}$
194 mass was characterized by elevated concentrations of Ca, Fe, Mg, Mn, Si, Sr indicative of haul road
195 dust, and 27% of the mass was elevated in both bitumen (V, Ni, S, Mo) and sand (Si, Al, Ti)
196 components indicative of a fugitive oil sand source. PMF resolved five $PM_{2.5}$ sources which explained
197 96% of the mass. $PM_{2.5}$ sources included contributions from oil sands upgrading (32% of fine PM mass
198 characterized by elevated SO_2, S, Mo, V, and Ni with negligible crustal element contributions), mixed
199 source fine fugitive dust (26%, elevated Al, Ca, Ce, Fe, La, Nb, Nd, Si, Sm, and Ti), biomass
200 combustion (25%, elevated Cd, K, Rb, Zn), with lesser contributions from a lead source (9%) and winter
201 road salt (4%). The temporal variation in the source contributions in the coarse and fine PM based on
202 the PMF results are presented in Figure 3a and b.
203
204 ***Fort McKay Ambient Dichotomous Sample Pb Isotope Results***
205 The $^{206}Pb/^{207}Pb$ and $^{208}Pb/^{207}Pb$ isotope ratios from all of the coarse and fine fraction PM samples from
206 Ft. McKay are plotted in Figure 4a. The coarse fraction samples plot in an elliptical field that in general
207 has higher $^{206}Pb/^{207}Pb$ and $^{208}Pb/^{207}Pb$ than the elliptical field that encompasses the fine fraction samples.
208 If one plots the coarse and fine results from the same sample collection day, the coarse fraction almost
209 always has higher $^{206}Pb/^{207}Pb$ and $^{208}Pb/^{207}Pb$ than the fine fraction (not shown here). Because the PM
210 sources that contribute to the coarse and fine PM differ based on the PMF source apportionment results
211 it is possible Pb isotopes might also impart a signature that reflects differences in PM sources. That
212 possibility is explored in the next section.
213
214 ***Results and Insights from Pb Isotopes from Source and Soil Samples from the AOSR***
215 Pb isotopes were measured on source samples from the AOSR from exposed (weathered) and fresh oil
216 sands, processed materials produced during the upgrading operations as well as the sand and clay from
217 tailings ponds, limestone from quarrying operations, access road materials, and PM from stacks and
218 heavy hauler fleets (Figure 4b). The PM source samples from upgrader stacks and the heavy hauler fleet
219 had been collected using dilution systems to allow aerosols to form via condensation and coagulation as
220 the exhaust stream cools to ambient temperature (Wang et al., 2012; Watson et al., 2012; Wang et al.,
221 2016). In addition, soils from lichen sample collection sites were collected and analyzed for Pb isotopes
222 as part of a prior study (Graney et al., 2017) and are included in Figure 4b.

223 The processed material and stack samples had the highest $^{208}Pb/^{207}Pb$ and $^{206}Pb/^{207}Pb$ ratios whereas the
224 fleet, tailings and soils had lower $^{208}Pb/^{207}Pb$ and $^{206}Pb/^{207}Pb$ ratios, with the weathered and fresh oil
225 sands displaying a wide range of Pb isotope ratios. The Pb isotopes from the oil sands samples plot in a
226 linear array that does not intersect the processed material and stack samples.

227 In the AOSR near source atmospheric pollution mainly consists of coarse fugitive PM emissions (wind-
228 blown dust) and fine PM diesel engine combustion exhaust from shovel and truck fleet operations
229 (Landis et al., 2012; Wang et al., 2015a; Wang et al., 2015b). Therefore the fine fraction PM near
230 mining operations likely contains a large component of combustion exhaust whereas the coarse fraction
231 PM contributions are likely a mixture from several fugitive dust sources.

232 We would expect the PM from the fleet samples (as well as the PM from other high temperature
233 combustion processes such as oil sands upgrading) to be $PM_{2.5}$ dominant whereas the oil sand,
234 limestone, and tailing sands would be predominantly in the $PM_{10\text{-}2.5}$ fraction (Landis et al., 2017). The
235 Pb isotope ratios from the dichot results reflect this expectation for results from the $PM_{2.5}$ are most
236 similar to values from the fleet samples, whereas the $PM_{10\text{-}2.5}$ is most similar to a mixture of the oil sand,
237 limestone, and tailing sands values (Figure 4ab). The dichot results do not suggest a large contribution
238 from AOSR stack emissions based on the extent of the ellipitical fields for either the coarse or fine Pb
239 isotope results. It is possible that the stack emissions would be reflected more in far field deposition
240 rather than near field deposition. Because the AMS-1 site in Fort MaKay is located proximal to several
241 of the mining and upgrading facilities PM at this site was expected to be heavily impacted by near field
242 sources. To assess far field deposition information from sites proximal and distal to mining operations
243 are needed.
244
245 ***Results and Insights from Pb Isotopes from Lichen Samples from the AOSR***

246 Lichen samples had been collected in the AOSR in 2008 to assess element and Pb isotope trends at 121
247 sites proximal and distal from mining operations (Edgerton et al., 2012; Graney et al., 2012). Based on
248 this previous work in the AOSR, it has been demonstrated that the Pb isotope composition of lichens is a
249 better indicator of source strength than Pb concentrations (Graney et al., 2012) The Pb isotope results
250 from the lichens collected in 2008 suggest a decrease in $^{206}Pb/^{207}Pb$ and $^{208}Pb/^{207}Pb$ from the near field
251 to distal sites (Figure 4c) suggesting a larger influence of $PM_{10\text{-}2.5}$ at the near field site, and a greater
252 contribution of $PM_{2.5}$ at the distal sites. The clustering of the results into the two groupings is similar to
253 the results from the dichots. The lichen results plot in ellipitical fields that have a smaller magnitude in

Pb isotope space than the dichot results. The width of the elliptical fields for the distal lichen samples and the fine PM dichot samples suggest there could be more variability in Pb isotope space, and hence sources and their signatures, than in the proximal lichens and coarse PM dichot samples.

Insights from Pb Isotopes from Aerosol Samples from other Studies

Particulate matter and lichen biomonitoring studies have identified the fugitive emission of coarse mode PM ($PM_{10-2.5}$) from oil sand production activities as the primary driver of the observed near field atmospheric deposition and spatial patterns in the AOSR (Landis et al., 2012, 2017). However the fine PM results indicate that there are other atmospheric emission sources superimposed over the coarse PM results. Specifically, the $PM_{2.5}$ lead source factor identified in the PMF source apportionment demonstrates a seasonal temporal trend (Figure 3a) with two primary episodes of enhanced Pb concentrations observed during the spring of 2010 and the spring of 2011. Other elements with significant loading on this factor were As, Zn, and Cd. This multi-element signature could reflect high temperature anthropogenic emission processes such as coal combustion or smelter emissions associated with long distance transport. If so Pb isotope measurements from aerosols from other regional and global scale studies might provide insights to document long range transport superimposed over local source contributions in the AOSR.

The Pb isotope results from aerosols collected in urban areas by Bollhöfer and Rosman (2001 and 2002) are presented in Fig. 4b. Samples from cities in China, Japan, Canada and the United States are included in this plot. Note that the US and Canada aerosols overlap in isotope space, with the US aerosols typically having higher $^{206}Pb/^{207}Pb$ and $^{208}Pb/^{207}Pb$ than the samples from Canada. Interestingly the samples from the cities in the US with the highest $^{206}Pb/^{207}Pb$ and $^{208}Pb/^{207}Pb$ are from coastal areas where oil fired power plants are located (i.e. Tampa Florida, Pancras et al., 2011). The samples from these coastal cities lie along a linear array that would intersect the source signature for samples from the stack and process samples from the AOSR. These samples likely represent the Pb isotope signature for synthetic oil from upgraded bitumen, and may be representative of the Pb isotope signature emitted by oil combustion processes. Note that the samples from China plot along a linear trend that is offset from the US and Canada field. Specifically the samples from China are offset in Pb isotope space along a trend that has a higher $^{208}Pb/^{207}Pb$ at similar $^{206}Pb/^{207}Pb$ values. This reflects a greater thorogenic component in the China samples in comparison to the US and Canada samples that has been noted in

several studies previously (Mukai et al., 1993, 1995; Bellis et al., 2005, Cheng and Hu, 2010). This Pb isotopic distinction has recently been used to quantify the contribution from China in aerosol samples collected in California (Ewing et al., 2010) as well as in ice from western Canada (Gross et al., 2012) and Greenland (Bory et al., 2014). If one examines the results from the $PM_{2.5}$ dichots and distal lichens from the AOSR in detail, one might postulate that there is also a contribution from combustion sources from China in these samples. The next section will attempt to quantify this contribution based on Pb isotope ratios and Pb concentrations in aerosols from the Ft. McKay site.

Quantifying Source Contributions in Fine PM Aerosol Samples from Pb Isotope Perspectives

If the $^{208}Pb/^{207}Pb$ versus $^{206}Pb/^{207}Pb$ results from the fine PM results are examined in detail, a triangular area that encompasses most of the results is found (Figure 5). It is possible that the apices of the triangle represent the endmember Pb isotope sources that mix together to result in the fine PM dichot results. The three endmembers include an isotope composition that "points toward" the fugitive dust from the AOSR (local sources), another endmember that points towards an isotopic composition similar to aerosols collected from cities in western Canada (regional source) and a third endmember that points towards emissions from eastern Asia, particularly cities in China (see below). If we assume that these three endmembers comprise the main sources of Pb in the aerosols collected in the AOSR, a three component mixing model can be used to determine the fractional contribution from the three sources on a sample by sample basis. The measurement of three isotopes of Pb (for example the ^{208}Pb, ^{207}Pb, and ^{206}Pb measured in this study) allow as many as three sources of Pb to be quantified (Gobeil et al., 1995). Pb isotope ratios using measurements from three isotopes of lead have been used previously to constrain Pb sources in sediments (Gobeil et al., 1995) and precipitation samples (Graney and Landis, 2012). The equations for the mixing model and the input parameters used in this study are found in Table 1. Note that the input parameters for the China source correspond to the average of the isotope ratios from the 4 cities in China (Figure 4d) reported in Bollhöfer and Rosman (2001). The input parameters for the Canadian source reflect contributions from cities in western Canada (Figure 4d) reported in Bollhöfer and Rosman (2001, 2002). The results from this three component source attribution are presented on a temporal basis in Figure 6ab and summarized in Table 1. Note that the contributions from China are most pronounced (in many cases over 50%) in April and May of 2010, and in January – May in 2011. This temporal relation matches the time of year in multi-element studies when trans-Pacific transport of aerosols is pronounced in North America (Fischer et al., 2009 and references therein). Overall sources from western Asia (China) contribute 47.1% of the Pb in the fine PM, local AOSR sources 27.0% and

315 western Canada 25.9 % based on the results from the Pb isotope ratio mixing model (Table 1) at Ft.
316 McKay over the 2010-2011 sampling timeframe.

317 ***Quantifying Source Contributions in Coarse PM Aerosol Samples from Pb Isotope Perspectives***

318 If the $^{208}Pb/^{207}Pb$ versus $^{206}Pb/^{207}Pb$ results from the coarse PM results are examined in detail, a
319 triangular area that encompasses most of the results can be constructed (Figure 7). Based upon PMF
320 results from prior studies (Landis et al., 2012, 2017), we would anticipate that the coarse PM would be
321 from local sources including oil sand, haul and access roads and tailings sand. Based on the Pb isotope
322 results from the AOSR source samples (Figure 4b), the three endmembers might include an isotope
323 composition that "points toward" fugitive dust from weathered and fresh oil sand, an endmember that
324 points towards an isotopic composition similar to tailings sand, and a third endmember that may be a
325 haul and access road signature (which would include a major contribution from limestone). If we
326 assume that the oil sand, haul roads and tailings sand are the three endmembers that comprise the main
327 sources of Pb in the coarse PM collected in the AOSR, a three component mixing model can once again
328 be used to determine the fractional contribution from the three sources on a sample by sample basis. The
329 model input parameters are found in Table 1, and the results from this source attribution are presented
330 on a temporal basis in Figure 8ab and summarized in Table 1. Overall the temporal results indicate
331 larger contributions from oil sand sources from March – October 2010 with tailings and road
332 contributions increasing after December 2010 until summer 2011, when oil sands again predominate.
333 Overall roads contribute 37.9% of the Pb in the coarse PM, oil sand 34.9% and tailings sand 27.2 %
334 based on the results from the Pb isotope ratio mixing model (Table 1) at Ft. McKay over the 2010-2011
335 sampling timeframe.

336 If one combines the results from the coarse and fine PM (Table 2), contributions from China (34.4%)
337 exceed those from mixed sources of fine PM from the AOSR (19.7 %), regional western Canada sources
338 of fine PM (19.0%), coarse PM from haul and access roads (10.2%), oil sands (9.4%) and tailings sand
339 (7.3%).

340

341 ***Quantifying Source Contributions in Lichen Samples from the AOSR from Pb Isotope Perspectives***

342 The *Hypgymnia physodes* lichens that were collected in 2008 are known to accumulate both coarse and
343 fine particulate matter (Graney et al., 2017). At present, the age of the lichens is unknown, and we
344 assume that they integrate and retain a longer term Pb isotope signal than the 16 month time frame over

345 which the PM that was collected at Ft. McKay. If the $^{208}Pb/^{207}Pb$ versus $^{206}Pb/^{207}Pb$ results from the
346 lichen results are examined in detail, a triangular area that encompasses most of the results is also found.
347 The three apices of the triangle point towards coarse PM from the AOSR (local source), a global source
348 from western Asia indicated by the fine PM results and a regional source from Canada that likely
349 includes fine PM from cities in western Canada and biomass combustion as well (Figure 9). Combustion
350 of biomass includes contributions from wildland fires as well as wood for heating residences in the
351 AOSR, and is a large contributor to the PMF source estimates (Figure 3b). The triangular field that
352 encloses the Pb isotope values from the lichens (Figure 9) has a slightly different global endmember
353 composition than the one used for the fine PM. Although a large contribution of Pb from China to the
354 lichens is likely, another source is needed to lower the $^{208}Pb/^{207}Pb$ and $^{206}Pb/^{207}Pb$ to an appropriate
355 endmember value to obtain good results from the isotope mixing model. An inclusion of emissions from
356 the mining and processing of the ore deposits in Kazakhstan (central Asia), the major source of Pb ore
357 used in Russia (Mukai, 2001) may contribute to the subtle shift in the Asian (global) Pb isotope
358 endmember composition depicted in Figure 9 versus Figure 7. Average $^{208}Pb/^{207}Pb$ and $^{206}Pb/^{207}Pb$ from
359 the main Pb ore deposit in Kazakhstan is 2.431 and 1.149 (Mukai, 2001) which would shift the Asian
360 source endmember to slightly lower Pb isotope values after mixing with anthropogenic Pb from China.
361 It is known that anthropogenic sources of Pb and other metals are entrained in the aerosol dust from
362 Asian deserts that is transported to North America. Based on results from several PM collection studies
363 in South Korea (Lee et al., 2013, 2015, 2016) the anthropogenic signature from Asian sources
364 overwhelms the signature from the natural Pb contained in the desert dust sources. So, the global
365 component in Figure 9 is likely a mixture of anthropogenic Pb from Kazakhstan (minor component) and
366 China (major component).

367 If the three Pb isotope endmembers calculations from the dichot results are applied in a similar manner
368 to the lichen data (see Table 1), an estimate of long term trans-Pacific transport of aerosols to the AOSR
369 can be obtained. If one uses the metric of distance from the oil sands operations to plot the Pb isotope
370 source contribution results, the more distal samples contain a greater contribution from sources in
371 western Asia. Stated in another way, even though lichens likely integrate the multi-source signals over
372 several years of PM transportation and deposition processes, a source contribution from China is
373 apparent. Overall regional sources contribute 51.7% of the Pb in the lichens, local sources 27.8% and
374 global sources 20.6% based on the results from the Pb isotope ratio mixing model (Table 1). However if
375 the mixing model results from the proximal lichens (0-30 km) and distal lichens (30-160 km) are

separated, local and regional sources predominate at the proximal sites, and global sources are more important at the distal sites (Table 2).

Other Insights from this Study

It should be noted that a contribution from bitumen upgrading processes in the AOSR was not apparent in the PM or lichen data sets. The contribution from biomass combustion may have been larger than anticipated reflecting both wildfire and heating sources, and needs to be characterized by further studies. The results from the distal lichen samples (Figure 4c) might best represent the long term Pb isotope source signature for Pb from combusted biomass mixed with western Asian sources. The integrated regional signal from western Canada sources likely includes transportation sources from far field urban sources but was difficult to quantify because the Pb isotopes from the fleet vehicle emissions in the AOSR are likely similar in composition. For the purpose of this analysis we assumed that the fleet vehicle signature represented a contribution in both the local and regional sources.

Conclusions

Daily twenty-four hour integrated fine ($PM_{2.5}$) and coarse ($PM_{10-2.5}$) particulate matter was collected using a sequential dichotomous sampler at Ft. McKay in the Athabasca Oil Sand Region in northeastern Alberta, Canada. A subset of 100 filter pairs were selected for element and Pb isotope analysis to determine short term variation in source contributions. Pb isotope results from 120 lichen samples collected in 2008 were also analyzed to examine longer term source contributions.

The results from measurements of $^{206}Pb/^{207}Pb$ and $^{208}Pb/^{207}Pb$ isotope ratios were used to identify local regional and global sources in the PM and lichen data sets. The key for identifying the global source was the recognition of thorogenic Pb from western Asia in three isotope $^{206}Pb/^{207}Pb$ versus $^{208}Pb/^{207}Pb$ plots.

Because the Pb concentrations in aerosols at Ft. McKay from local sources were low, it proved to be feasible to determine contributions from local, regional and global sources through use of Pb isotope ratios coupled with a three source mixing model for the fine and coarse PM and lichen data sets.

If one combines the results from the coarse and fine PM, contributions from China (34.4%) exceed those from mixed sources of fine PM from the AOSR (19.7 %), regional western Canada sources of fine PM (19.0%), and coarse PM from haul and access roads (10.2%), oil sands (9.4%) and tailings sand (7.3%) sources.

405 Regional sources contribute 51.7% of the Pb in the lichens, local sources 27.8% and global sources
406 20.6%. If the mixing model results from the proximal lichens (0-30 km) and distal lichens (30-160 km)
407 are separated, local and regional sources predominate at the proximal sites, and global sources are more
408 important at the distal sites. the ratios associated with many of these spring episodes are consistent with
409 lead of Asian origin.

410 The long range transport of Pb from western Asia sources is superimposed over local PM sources in the
411 AOSR. It is remarkable that we could identify and quantify the amount of this global transport signature
412 in a location within the footprint of the world's largest concentration of bitumen mining and upgrading
413 facilities.

414

415 **Acknowledgements:** This work was funded by the Wood Buffalo Environmental Association
416 (WBEA). The content and opinions expressed by the authors do not necessarily reflect the views of the
417 WBEA or of the WBEA membership. We thank Gary Cross (WBEA) for managing the ambient sample
418 collection activities in the AOSR; Sanjay Prasad (WBEA) for providing AMS-1 Fort McKay monitoring
419 site ancillary ambient measurement data used in our analysis; Zack Eastman, Hayley Drake, and Kendra
420 Thomas (WBEA) for ambient sample support; Brad Edgerton (ARA) for filter weighing and logistics,
421 and Mike Fort (ARA) for dichotomous sampler filter extraction and ED-XRF and DRC-ICPMS
422 analysis. We thank Allan Legge, Kevin Percy, Keith Puckett and William Studabaker for their insights
423 and constructive reviews of the early versions of this manuscript.

424 **Literature Cited**

425 Attanasi, E.D.; Meyer, R.F., 2010. Natural Bitumen and Extra-Heavy Oil - Survey of energy resources
426 (22 ed.). World Energy Council, 123–140. ISBN 0-946121-26-5

427 Bellis, J.D., Satake, K., Inagaki,M., Zeng, J., Oizumi, T., 2005. Seasonal and long-term change in lead
428 deposition in central Japan: evidence for atmospheric transport from continental Asia. Sci. Total
429 Environ. 341, 149–158.

430 Bollhöfer, A., Rosman, K.J.R., 2001. Isotopic signatures for atmospheric lead: the Northern
431 Hemisphere. Geochim. Cosmochim. Acta 65, 1727–1740.

432 Bollhöfer, A., Rosman, K.J.R., 2002 The temporal stability in lead isotopic signatures at selected sites in
433 the Southern and Northern Hemispheres. Geochim. Cosmochim. Acta 66, 1375–1386.

434 Bory, A.J.M., Abouchami, W., Galer, S.J.G., Svensson, A., Christensen, J.N., Biscaye, P.E., 2014. A
435 Chinese imprint in insoluble pollutants recently deposited in central Greenland as indicated by lead
436 isotopes. Environ. Sci. Technol. 48, 1451−1457.

437 Chen J., Tan M., Li Y., Zhang Y., Lu W., Tong Y., Zhang G., Li Y., 2005. A lead isotope record of

438 Shanghai atmospheric lead emissions in total suspended particles during the period of phasing out of
439 leaded gasoline. Atmos. Environ. 39, 1245–1253.

440 Chen, J., Tan, M., Li, Y., Zheng, J., Zhang, Y., Shan, Z., Zhang, G., Li, Y., 2008. Characteristics of trace
441 elements and lead isotope ratios in PM2.5 from four sites in Shanghai. J. Hazard. Mater. 156, 36–43.

442 Cheng, H., Hu, Y., 2010. Lead (Pb) isotopic fingerprinting and its applications in lead pollution studies
443 in China: a review. Environ. Pollut. 158, 1134–1146.

444 Edgerton, E.S.; Fort, J.M.; Baumann, K.; Graney, J.R.; Landis, M.S.; Berryman, S.; Krupa, S., 2012.
445 Method for Extraction and Multi-element Analysis of *Hypogymnia physodes* Samples from the
446 Athabasca Oil Sands Region. In Alberta Oil Sands: Energy, Industry and the Environment, pp. 315-
447 342. Kevin Percy ed., Elsevier, Oxford, England.

448 Ewing, S.A., Christensen, J.N., Brown, S.T., Vancuren, R.A., Cliff, S.S., Depaolo, D.J., 2010. Pb
449 isotopes as an indicator of the Asian contribution to particulate air pollution in urban California.
450 Environ. Sci.Technol. 44, 8911−8916.

451 Fischer, E.V., Hsu, N.C., Jaffe, D.A., Jeong, M.-J., Gong, S.L., 2009. A decade of dust:
452 Asian dust and springtime aerosol load in the U.S. Pacific Northwest. Geophys. Res. Lett. 36, L03821

453 Gallon, C.; Ranville, M.A.; Conaway, C.H.; Landing, W.M.; Buck, C.S.; Morton, P.L.; Flegal, A.R.,
454 2011. Asian industrial lead inputs to the north Pacific evidenced by lead concentrations and isotopic
455 compositions in the surface waters and aerosols. Environ. Sci. Technol., 45, 9874–9882.

456 Gobeil, C., Johnson, W.K., MacDonald, R.W., Wong, C.S., 1995. Sources and burden of lead in St.
457 Lawrence Estuary sediments: isotopic evidence. Environ. Sci. Technol. 29, 193–201.

458 Graney, J.R., Landis, M.S., Krupa, S., 2012. Coupling lead isotopes and element concentrations in
459 epiphytic lichens to track sources of air emissions in the Athabasca Oil Sands Region. In Alberta Oil
460 Sands: Energy, Industry and the Environment, pp. 343-372. Kevin Percy ed., Elsevier, Oxford,
461 England.

462 Graney, J.R.; Landis, M.S.; Puckett, K.J.; Studabaker, W.; Edgerton, E.S.; Legge, A.; Percy, K.E. 2017.
463 Differential accumulation of PAHs, elements, and Pb isotopes by five lichen species from the Athabasca
464 oil sands region in Alberta, Canada. Chemosphere, 184, 700-710.

465 Gross, B.H., Kreutz, K.J., Osterberg, E.C., McConnell, J.R., Handley, M., Wake, C.P., Yalcin, K., 2012.
466 Constraining recent lead pollution sources in the North Pacific using ice core stable lead isotopes. J.
467 Geophysical Res. 117, D16307.

468 Hosono, T., Alvarez, K., Kuwae, M., 2016. Lead isotope ratios in six lake sediment cores from Japan
469 Archipelago: Historical record of trans-boundary pollution sources. Sci. Total Environ. 559, 24-37.

470 Huang, R., McPhedran, K.N., Yang, L., Gamal El Din, M., 2016. Characterization and distribution of
471 metal and nonmetal elements in the Alberta oil sands region of Canada. Chemosphere, 147, 218-229.

472 Jaffe, D., Anderson, T., Covert, D., Kotchenruther, R., Trost, B., Danielson, J., Simpson,
473 W., Berntsen, T., Karlsdottir, S., Blake, D., Harris, J., Carmichael, G., Itsushi, U.,
474 1999. Transport of Asian air pollution to North America. Geophys. Res. Lett. 26, 711–714.

475 Jalkanen, L.M.; Häsänen, E.K. 1996. Simple Method for the Dissolution of Atmospheric Aerosol
476 Samples for Analysis by Inductively Coupled Plasma Mass Spectrometry. Journal of Analytical Atomic
477 Spectrometry, 11, 365-369.

478 Jones, C.E., Halliday, A.N., Rea, D.K., Owen, R.M., 2000. Eolian inputs of lead to the North Pacific.
479 Geochim. Cosmochim. Acta 64, 1405–1416.

480 Kong, S., Ji, Y., Lu, B., Chen, L., Han, B., Li, Z., Bai, Z., 2011. Characterization of PM10 source
481 profiles for fugitive dust in Fushun – a city famous for coal. Atmos. Environ. 45, 5351-5365.

482 Krachler, M., Le Roux, G., Kober, B., Shotyk, W., 2004. Optimising accuracy and precision of lead
483 isotope measurement (^{206}Pb, ^{207}Pb, ^{208}Pb) in acid digests of peat with ICP-SMS using individual mass
484 discrimination correction. Journal of Analytical Atomic Spectrometry 19, 354 – 361.

485 Landis, M.S.; Pancras, J.P.; Graney, J.R.; Stevens, R.K.; Percy, K.E.; Krupa, S. (2012). Receptor
486 Modeling of Epiphytic Lichens to Elucidate the Sources and Spatial Distribution of Inorganic Air
487 Pollution in the Athabasca Oil Sands Region. In Alberta Oil Sands: Energy, Industry and the
488 Environment, pp. 427-467. Kevin Percy ed., Elsevier, Oxford, England.

489 Landis, M.S., Pancras, J.P., Graney, J.R., White, E., Legge, A., Percy, K.E., 2017. Source
490 Apportionment of ambient fine and coarse particulate matter in Fort McKay, Alberta, Canada. Science
491 of the Total Environment, 584-585, 105-117.

492 Lee, P.-K., Youm, S.-J., Jo, H.Y., 2013. Heavy metal concentrations and contamination levels from
493 Asian dust and identification of sources: a case-study. Chemosphere 91, 1018–1025.

494 Lee, P.K., Jo, H.Y., Kang, M.J., Kim, S.O., 2015. Seasonal variation in trace element concentrations and
495 Pb isotopic composition of airborne particulates during Asian dust and non-Asian dust periods in
496 Daejeon, Korea. Environ. Earth Sci. 74, 3613 - 3628.

497 Lee, P.K., Yu, S., 2016. Lead isotopes combined with a sequential extraction procedure for source
498 apportionment in the dry deposition of Asian dust and non-Asian dust. Environ. Pollut. 210, 65-75.

499 Li, Q., Cheng, H., Zhou, T., Lin, C., Guo, S., 2012. The estimated atmospheric lead emissions in China.
500 Atmos. Env. 60, 1e8.

501 Loo, B.W; Cork, C.P., 1998. Development of High Efficiency Virtual Impactors. Aerosol Sci. Technol.
502 9, 167-176.

503 McFarland, A.R.; Ortiz, C.A.; Bertch Jr, R.W., 1978. Particle collection characteristics of a single stage
504 dichotomous sampler. Environ. Sci. Technol. 12, 679-682.

505 Mukai, H., Furuta, N., Fujii, T., Ambe, Y., Sakamoto, K., Hashimoto, Y., 1993. Characterizations of
506 sources of lead in the urban air of Asia using ratios of stable lead isotopes. Environ. Sci. Technol. 27,
507 1347–1356.

508 Mukai, H., Tanaka, A., Fujii, T., Zeng, Y., Hong, Y., 2001. Regional characteristics of sulfur and lead
509 isotope ratios at several Chinese urban sites. Environ. Sci. Technol. 35, 1064–1071.

510 Mukai, H., Machida, T., Tanaka, A., Pavel Vera, Y., Uematsu, M., 2001. Lead isotope ratios in the
511 urban air of eastern and central Russia. Atmos. Environ. 35, 2783–2793.

512 Ondov, J.M.; Wexler, A.S., 1998. Where do particulate toxins reside? An improved paradigm for the
513 structure and dynamics of the urban mid-Atlantic aerosol. Environ. Sci. Technol. 32, 2547–2555.

514 Osterberg, E.C., Mayewski, P., Kreutz, K., Fisher, D., Handley, M., Sneed, S., Zdanowicz, C., Zheng, J.,
515 Demuth, M., Waskiewicz, M., Bourgeois, J., 2008. Ice core record of rising lead pollution in the North
516 Pacific atmosphere. Geophysical Research Letters 35, L05810, 427 doi:05810.01029/02007GL032680.

517 Pancras, J.P., Vedantham, R., Landis, M.S., Norris, G.A., Ondov, J.M., 2011. Application of EPA unmix

518 and nonparametric wind regression on high time resolution trace elements and speciated mercury in
519 Tampa, Florida aerosol. Environ. Sci. Technol. 45, 3511–3518.

520 Percy, K.E., 2013. Ambient Air Quality and Linkage to Ecosystems in the Athabasca Oil Sands, Alberta.
521 Geoscience Canada, 40, 182-201.

522 Schleicher, N., Norra, S., Chai, F., Chen, Y., Wang, S., Cen, K., Yu, Y., Stüben, D., 2011. Temporal
523 variability of trace metal mobility of urban particulate matter from Beijing-A contribution to health
524 impact assessments of aerosols. Atm. Environ. 45, 7248-7265.

525 Shotyk, W., Bicalho, B., Cuss, C. W., Duke, M. J. M., Noernberg, T., Pelletier, R., Steinnes, E.,
526 Zaccone, C. 2016. Dust is the dominant source source of "heavy metals" to peat moss (*Sphagnum*
527 *fuscum*) in the bogs of the Athabasca Bituminous Sands region of northern Alberta. Environ. Int. 92,
528 494-506.

529 Shotyk, W., Appleby, P.G., Bicalho, B., Davies, L.J., Froese, D., Grant-Weaver, I., Magnan, G., Mullan-
530 Boudreau, G., Noernberg, T., Pelletier, R., Shannon, B., van Bellen, S., Zaccone, C. 2017. Peat bogs
531 document decades of declining atmospheric contamination by trace metals in the Athabasca Bituminous
532 Sands region. Environ. Sci. Technol. 51, 6237–6249.

533 Simonetti, A., Gariépy, C., Carignan, J., 2003. Tracing sources of atmospheric pollution in western
534 Canada using Pb isotopic composition and heavy metal abundances in epiphytic lichens. Atmospheric
535 Environment 37, 2853–2865.

536 Tan, M.G., Zhang, G.L., Li, X.L., Zhang, Y.X., Yue, W.S., Chen, J.M., Wang, Y.S., Li, A.G., Li, Y.,
537 Zhang, Y.M., Shan, Z.C., 2006. Comprehensive study of lead pollution in Shanghai by multiple
538 techniques. Anal. Chem. 78, 8044 - 8050.

539 Uematsu, M., Duce, R.A., Prospero, J.M., Chen, L., Merrill, J.T., McDonald, R.L., 1983. Transport of
540 mineral aerosol from Asia over the North Pacific Ocean. J. Geophys. Res. 88, 5343–5352.

541 U.S. Environmental Protection Agency. The 2011 National Emissions Inventory, Version 2. March
542 2015. Office of Air Quality Planning and Standards, Research Triangle Park, NC, USA. Last Accessed
543 April 1, 2016. https://www3.epa.gov/ttn/chief/net/2011inventory.html.

544 VanCuren, R.A.; Cahill, T.A., 2002. Asian aerosols in North America: Frequency and concentration of
545 fine dust. J. Geophys. Res., 107, 4804.

546 VanCuren, R.A., 2003. Asian aerosols in North America: Extracting the chemical composition and mass
547 concentration of the Asian continental aerosol plume from long-term aerosol records in the western
548 United States. J. Geophys. Res. Atmospheres, 108, 4263.

549 Wang,W., Liu, X., Zhao, L., Guo, D., Tian, X., Adams, F., 2006. Effectiveness of leaded petrol phase-
550 out in Tianjin, China based on the aerosol lead concentration and isotope abundance ratio. Sci. Total
551 Environ. 364, 175–187.

552 Wang, P., Cao, J., Shen, Z., Han, Y., Lee, S., Huang, Y., Zhu, C., Wang, H., Huang, R., 2015. Spatial
553 and seasonal variations of PM2.5 mass and species during 2010 in Xian China. Sci. Total Environ. 508,
554 477 -487.

555 Wang, X.; Chow, J.C.; Kohl, S.D.; Percy, K.E., Legge, A.H.; Watson, J.G., 2015. Characterization of
556 $PM_{2.5}$ and PM_{10} fugitive dust source profiles in the Athabasca Oil Sands Region. J. Air Waste Manag.
557 65, 1421 – 1433.

Wang, X.; Chow, J.C.; Kohl, S.D.; Percy, K.E.; Legge, A.H.; Watson, J.G., 2016. Real-world emission factors for Caterpillar 797B heavy haulers during mining operations. Particuology 28, 22-30.

Widory, D., Liu, X., Dong, S., 2010. Isotopes as tracers of sources of lead and strontium in aerosols (TSP & PM2.5) in Beijing. Atmos. Environ. 44, 3679 – 3687.

Yienger, J.J.; Galanter, M.; Holloway, T.A.; Phadnis, M.J.; Guttikunda, S.K.; Carmichael, G.R.; Moxim, W.J.; Levy II, H., 2000. The episodic nature of air pollution transport from Asia to North America. J. Geophys. Res. 106, 26931-26945.

Yip, Y.; Chung-wah Lamb, J.; Tong, W., 2008. Applications of lead isotope ratio measurements. Trends in Analytical Chemistry 27, 460-480.

Zdanowicz, C., Hall, G., Vaive, J., Amelin, Y., Percival, J., Girard, I., Biscaye, P., Borys, A., 2006. Asian dustfall in the St. Elias Mountains, Yukon, Canada. Geochim. Cosmochim. Acta, 70, 3493–3507.

Zheng, J., Tan, M., Shibata, Y., Tanaka, A., Li, Y., Zhang, G., Zhang, Y., Shan, Z., 2004. Characteristics of lead isotope ratios and elemental concentrations in PM10 fraction of airborne particulate matter in Shanghai after the phase-out of leaded gasoline. Atmos. Environ. 38, 1191–1200.

Zhou, S., Davy, P.K., Wang, X., Cohen, J.B., Liang, J., Huang, M., Fan, Q., Chen, W., Chang, M., Ancelet, T., Trompetter, W.J., 2016. High time-resolved elemental components in fine and coarse particles in the Pearl River Delta region of Southern China: Dynamic variations and effects of meteorology. Sci. Total Environ. 572, 634-648.

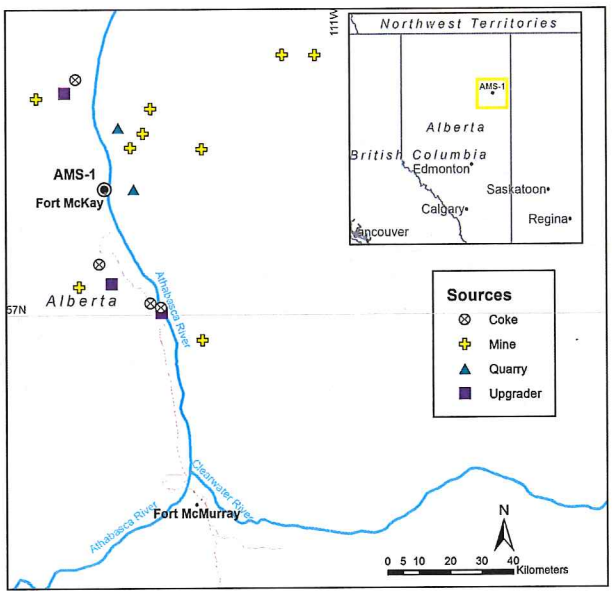

Figure 1. Map depicting the location of the WBEA AMS-1 Fort McKay ambient monitoring station in relation to major oil sand mining and production facilities in northeastern Alberta, Canada (inset). (update this…with outline of mine footprints superimposed over 2008 lichen collection locations)

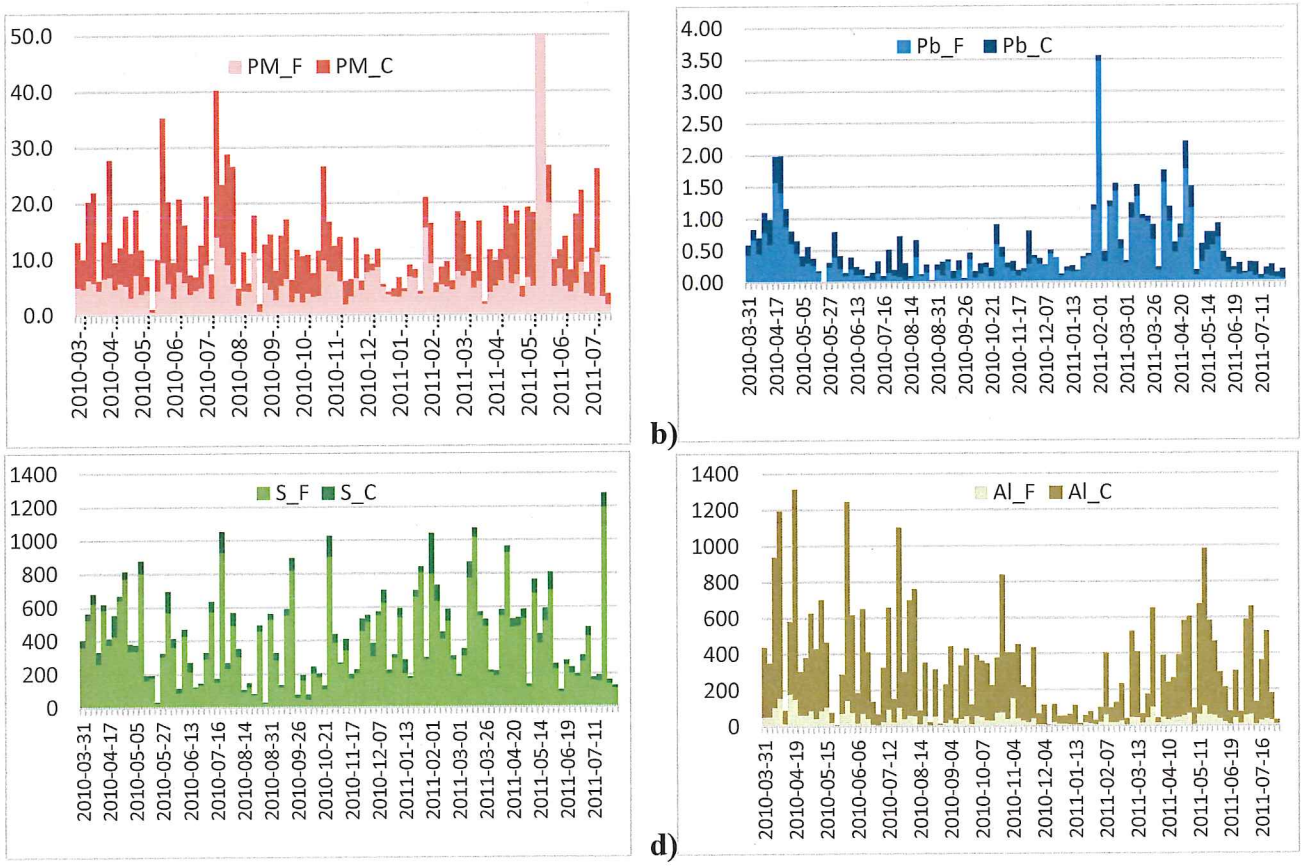

Figure 2. Temporal concentration results from the coarse (C) and fine fraction (F) dichot samples collected from Ft. McKay in 2010 and 2011. a) Coarse and Fine Total Particulate Matter (PM) concentrations in ug m^{-3} b) Lead (Pb) c) Sulfur (S) and d) Aluminum (Al) results in ng m^{-3}.

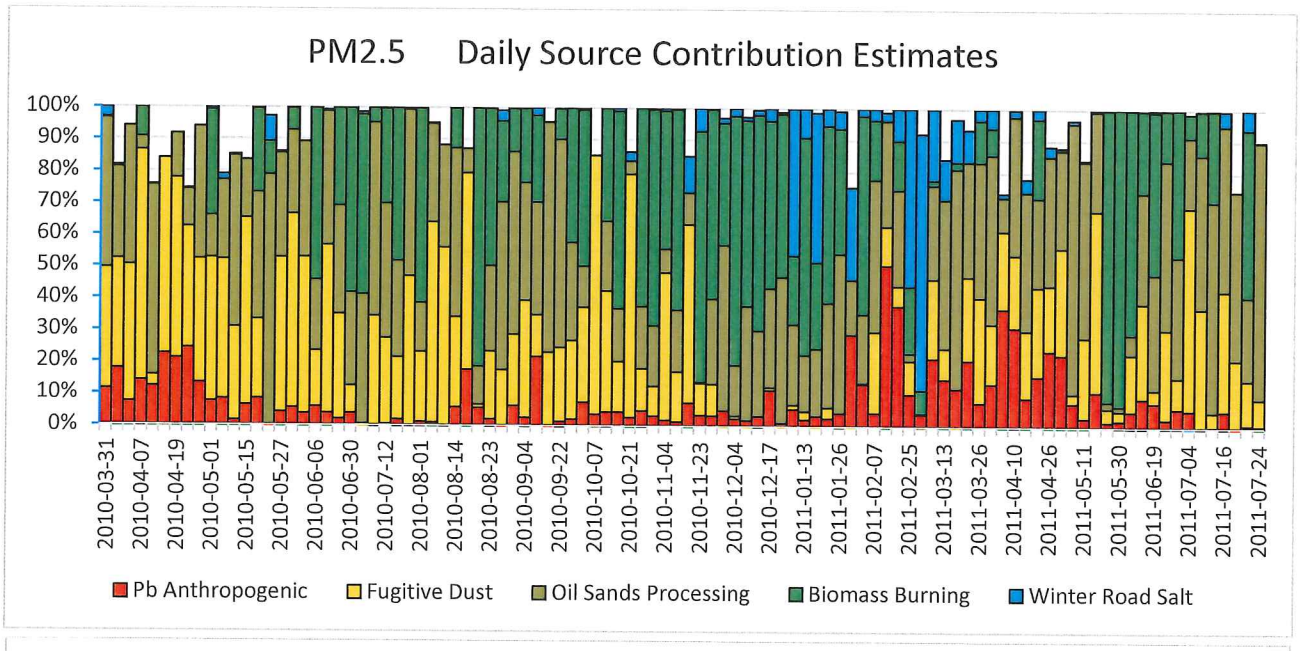

587 a)

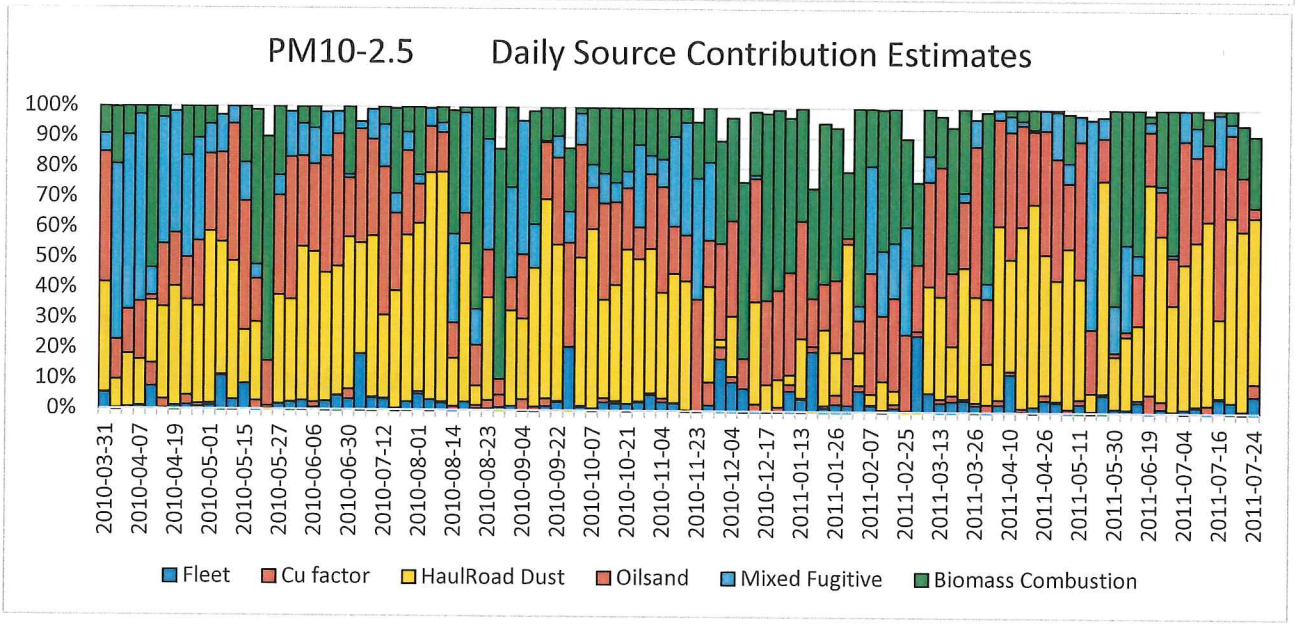

588 b)

589

590 **Figure 3.** PMF source contributions estimate time series from the AOSR Ft. Mackay AMS-1 site for a)
591 $PM_{2.5}$ and b) $PM_{10\text{-}2.5}$

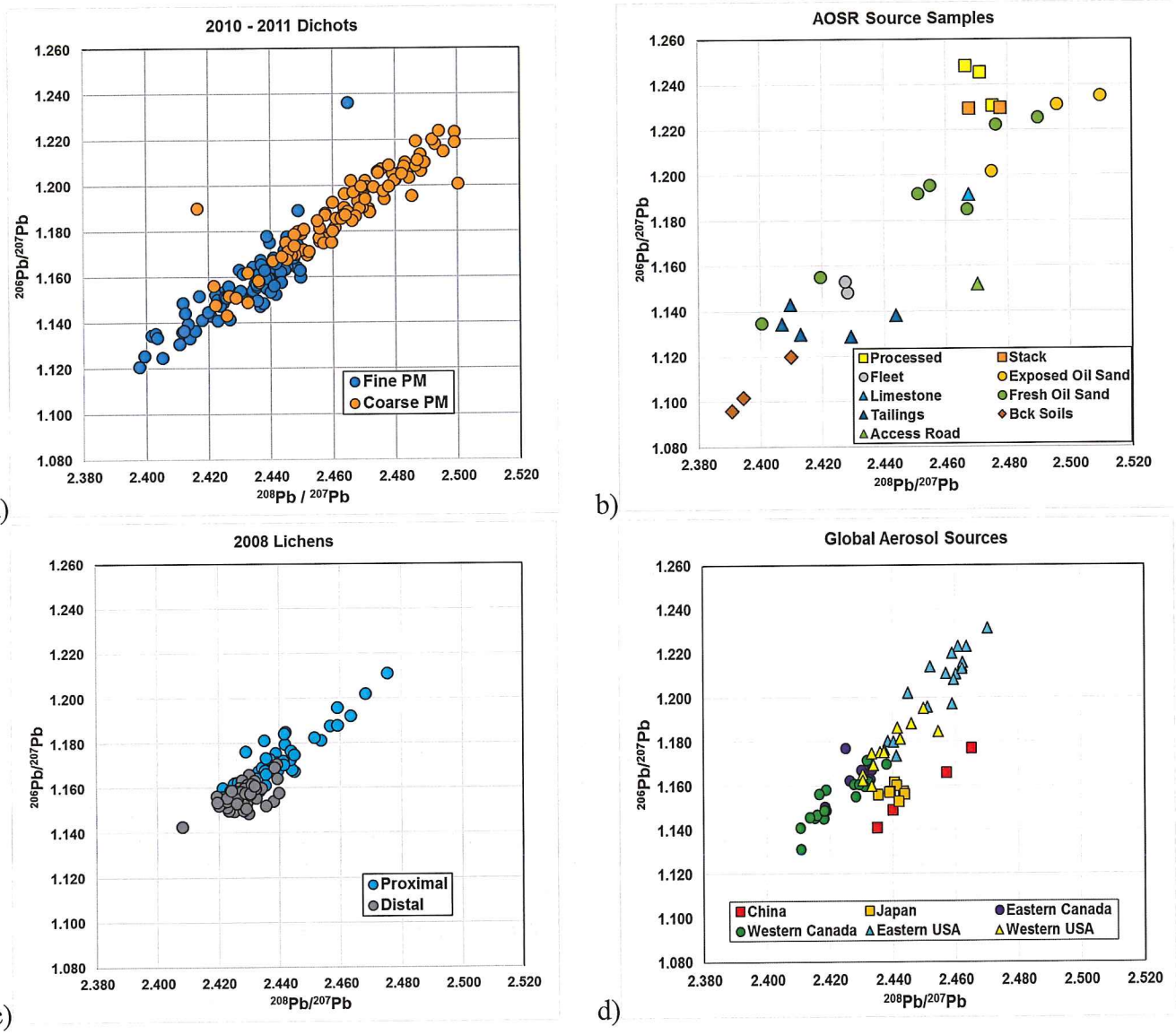

Figure 4. Pb isotope results from a) all of the dichot samples collected in 2010- 2011 at Ft. McKay, b) source samples from the AOSR, c) lichens collected in 2008 at sites proximal (< 30 km) and distal (30-160 km) from oil sands mining operations, and d) aerosols from China, Japan, Canada, and the United States (compiled from Bollhöfer and Rosman 2001, 2002 datasets).

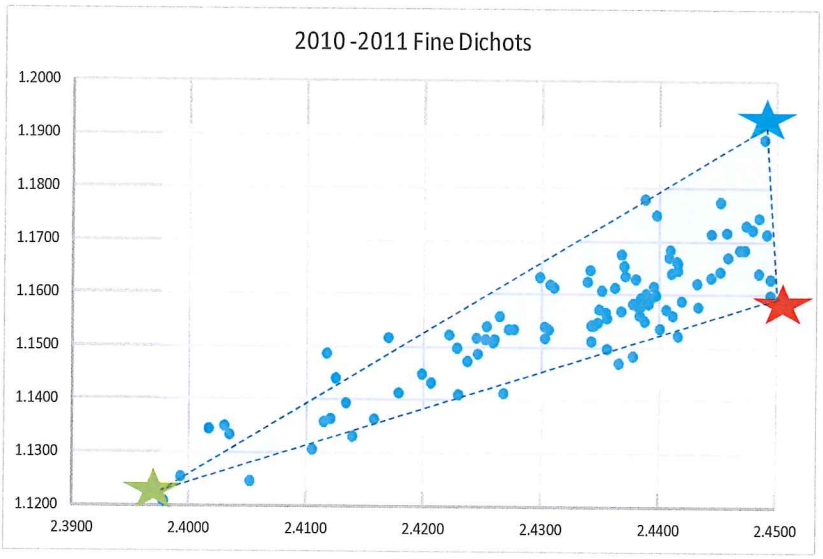

Figure 5. Pb isotope results from the fine fraction PM from Ft. McKay with proposed fine PM endmember compositions from local (AOSR, blue star), regional (western Canada, green star) and global (China, red star) sources. The triangle encloses the Pb isotope ratios from the samples within the three endmember spatial field.

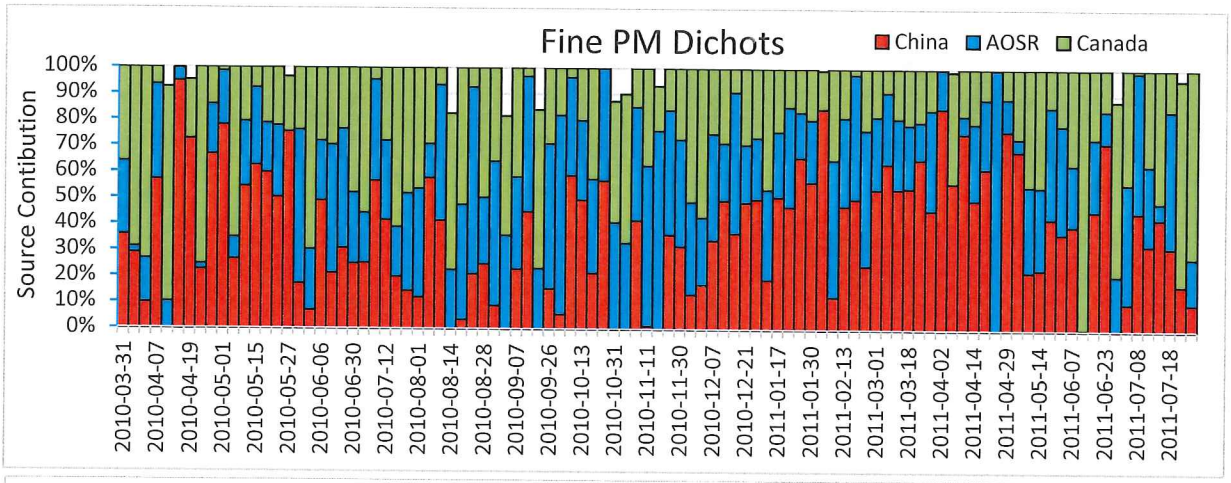

a)

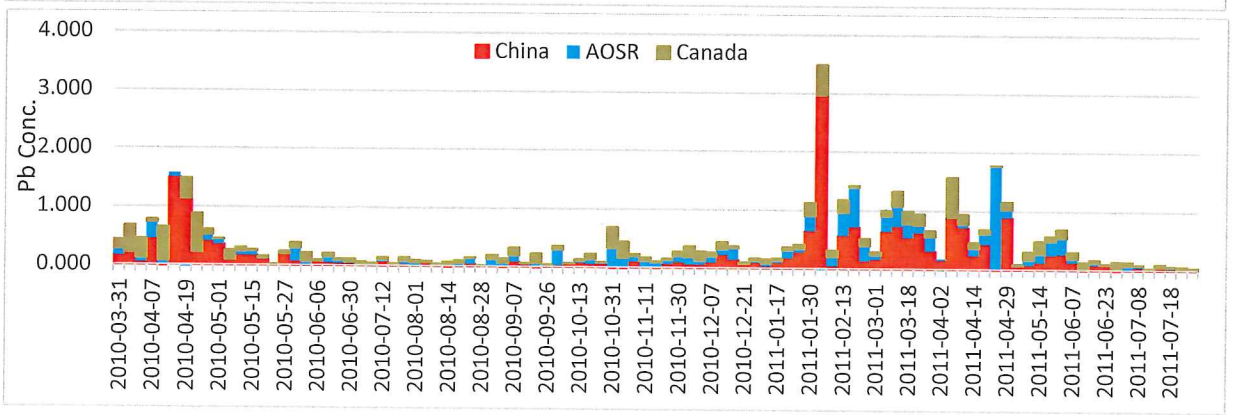

b)

Figure 6. Temporal fine PM a) percentage and b) Pb concentration contributions from local (AOSR), regional (Canada) and global (China) sources based on three component Pb isotope ratio and concentration mixing model.

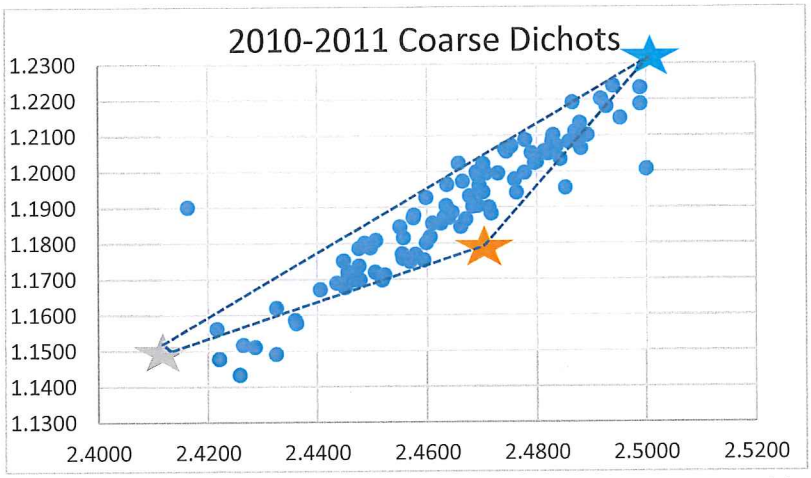

Figure 7. Pb isotope results from the coarse fraction PM from Ft. McKay with proposed coarse PM endmember compositions from AOSR sources including oil sand (blue star), tailings (gray star) and haul and access roads (brown star) sources. The triangle encloses the Pb isotope ratios from the samples within the three endmember spatial field.

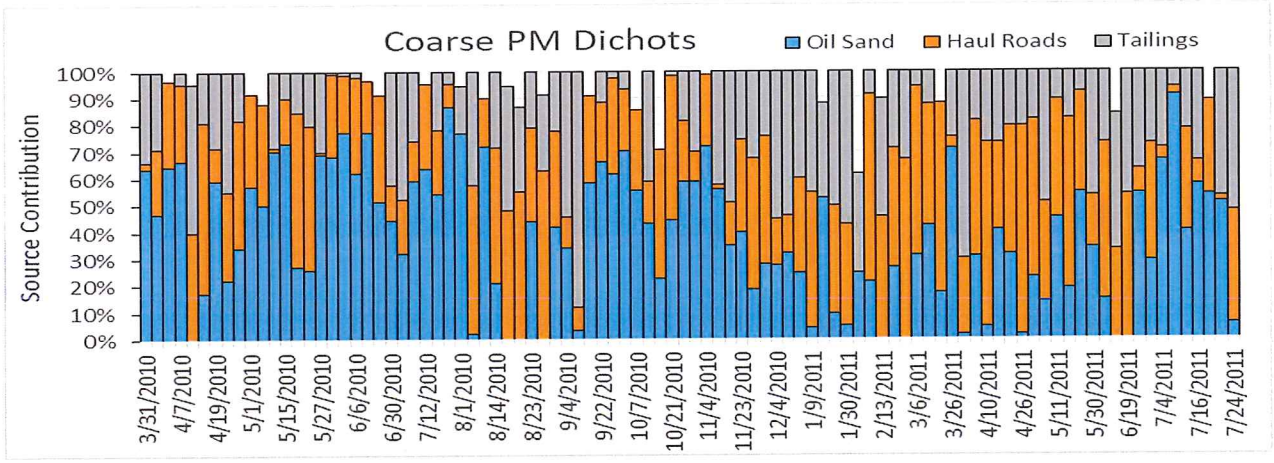

a)

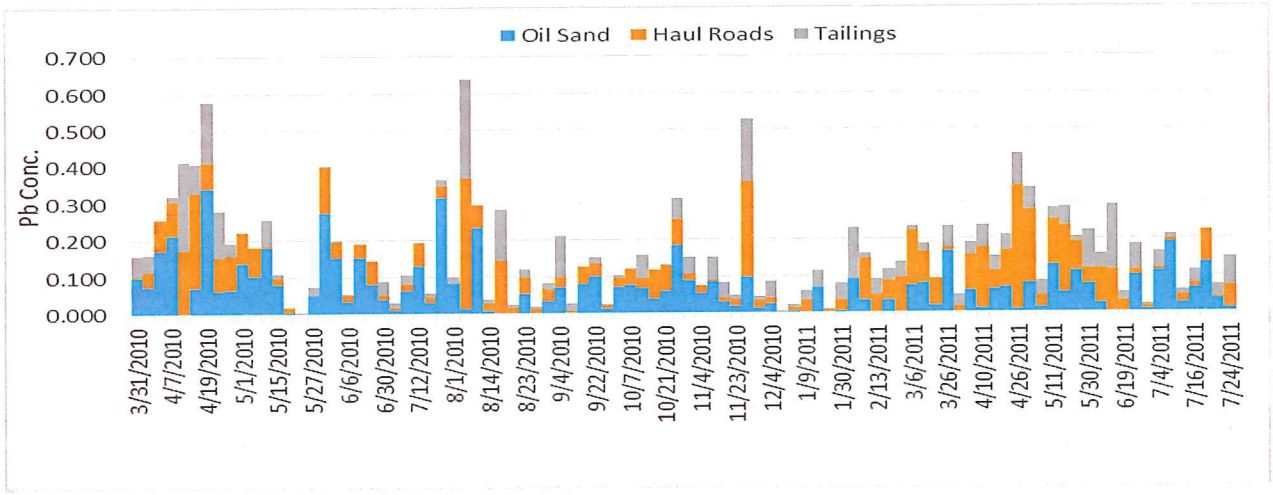

b)

Figure 8. Temporal coarse PM a) percentage and b) Pb concentration contributions from AOSR sources including oil sand, haul roads, and tailings sand based on three component Pb isotope ratio and concentration mixing model.

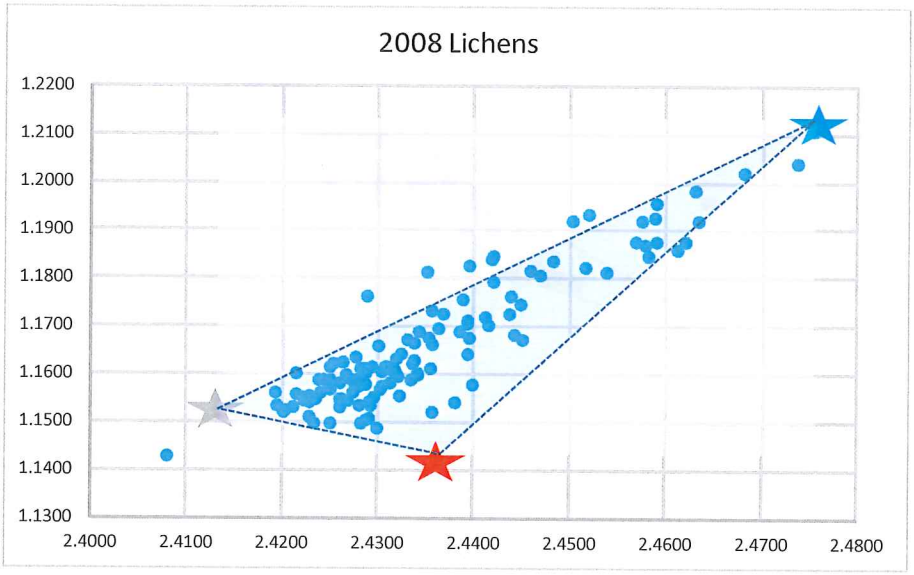

Figure 9. Pb isotope results from lichens from the AOSR with proposed endmember compositions from local (coarse PM AOSR fugitive dust, blue star), regional (Canada, grey star) and global (western Asia, red star) sources. The triangle encloses the Pb isotope ratios from the samples within the three endmember spatial field.

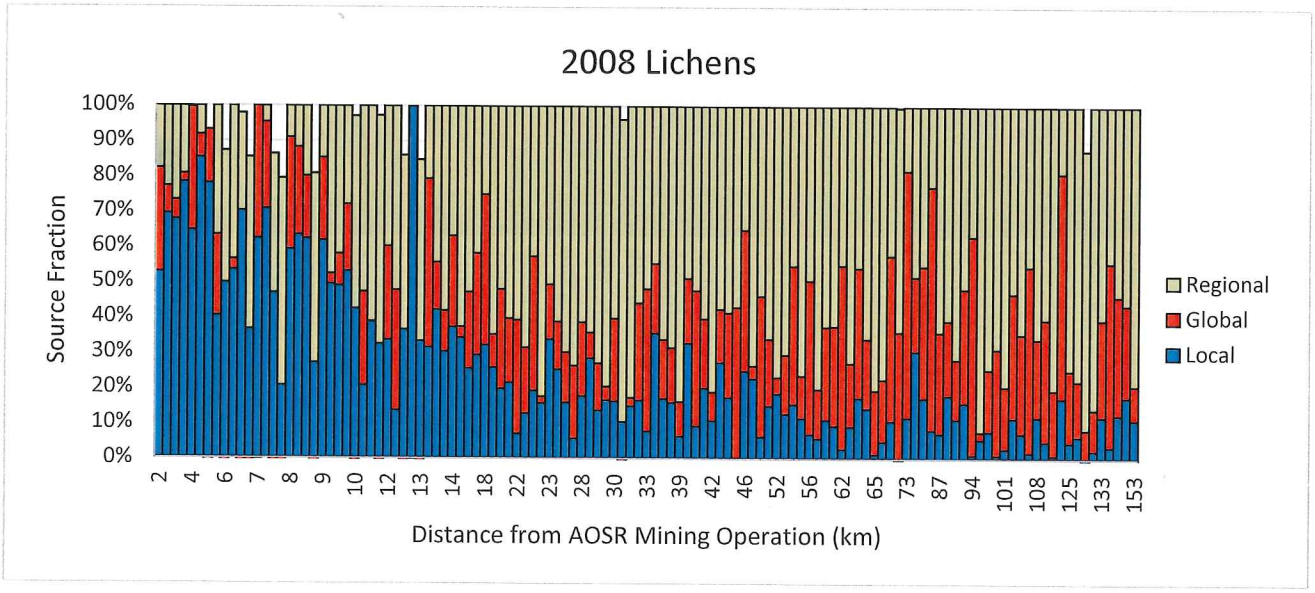

Figure 10. Lichen percentage contributions from regional (Canada), global (western Asia) and local (AOSR) sources based on three component Pb isotope ratio mixing model portrayed as a function of lichen sampling site distance from the nearest AOSR mining operation.

634

Table 1: Three Pb Isotope Source Mixing Model Parameters and Results

Equations

F1+F2+F3=1

aF1+bF2+cF3=d

eF1+fF2+gF3=h

Solutions

F3= ((h-e)(b-a)-(d-a)(f-e))/((g-e)(b-a)-(c-a)(f-e))

F2=((d-a)-F3(c-a))/b-a

F1=1-F2-F3

Model Input Parameters						Results Summary		
Source	Fine PM		208Pb/207Pb		206Pb/207Pb	Conc sum	%	Source
AOSR	F1	a=	2.449	e=	1.189	11.138	27.0	AOSR
China	F2	b=	2.449	f=	1.158	19.459	47.1	China
Canada	F3	c=	2.398	g=	1.121	10.722	25.9	Canada
	mixture	d=	variable	h=	variable	41.318	100.00	Total
Source	Coarse PM		208Pb/207Pb		206Pb/207Pb	Conc sum	%	Source
Oil Sand	F1	a=	2.500	e=	1.230	5.309	34.9	Oil Sand
Roads	F2	b=	2.470	f=	1.180	5.777	37.9	Roads
Tailings Sand	F3	c=	2.416	g=	1.153	4.144	27.2	Tailings
	mixture	d=	variable	h=	variable	15.230	100.00	Total
Source	Lichens		208Pb/207Pb		206Pb/207Pb	Conc sum	%	Source
Local	F1	a=	2.476	e=	1.211	99.777	27.8	Local
Global	F2	b=	2.438	f=	1.145	73.793	20.6	Global
Regional	F3	c=	2.416	g=	1.153	185.486	51.7	Regional
	mixture	d=	variable	h=	variable	359.057	100.0	Total

Each set of isotope ratios from the fine and coarse PM and lichen datasets was used for model input
The individual results are displayed on temporal plots of % source contributions.
The results summary summed the concentration contributions to provide overall source estimates.

635
636

Table 2: Source Attribution Summary

Combined PM Results

PM Pb Conc Sum	PM % Pb Source	Source
19.46	34.4	China (Global) Fine PM
11.14	19.7	AOSR Mixed Fine PM
10.72	19.0	Canada (Regional) Fine PM
5.78	10.2	AOSR Roads Coarse PM
5.31	9.4	AOSR Oil Sand Coarse PM
4.14	7.3	AOSR Tailings Coarse PM
56.55	100.0	sum

Lichen Results

Proximal (0-30 km)

Lichen Pb Conc sum	Lichen % Source	Source
83.09	43.7	Local
81.52	42.9	Regional
25.48	13.4	Global
190.09	100.0	sum

Distal (30-160 km)

Lichen Pb Conc sum	Lichen % Source	Source
103.96	61.5	Regional
48.32	28.6	Global
16.69	9.9	Local
168.97	100.0	sum

637